The International Journal of Advanced Manufacturing Technology (2022) 121:4625–4641
https://doi.org/10.1007/s00170-022-09677-0

ORIGINAL ARTICLE

Proposal of "relative Young's modulus" and its influence on cutting performance of abrasive suspension jet

Chiheng Qiang[1] · Kaining Yang[1] · Shinichi Warisawa[2] · Chuwen Guo[1]

Received: 19 October 2021 / Accepted: 3 July 2022 / Published online: 8 July 2022

Abstract

The Young's modulus of abrasive and the material to be cut will have different influences on the cutting performance of the abrasive suspension jet (ASJ). It is found that the relative ratio of their Young's modulus seems to show a better law on cutting performance of ASJ. In this paper, the concept of relative Young's modulus was proposed, the influence of relative Young's modulus on cutting performance of ASJ was explored, and the experiment of the influence of relative Young's modulus on the kerf depth and surface roughness of ASJ was carried out. The results showed that the kerf depth increases with the increase of relative Young's modulus. When the value is larger than 1, the density of the abrasive is the main factor affecting the kerf depth. When the value is smaller than 1, the Young's modulus of the abrasive is the main factor affecting the kerf depth. The surface quality is divided into three degrees according to roughness. When the relative Young's modulus is smaller than 1.5, it is a poor erosion degree. When the relative Young's modulus is between 1.5 and 4, it is the best quality degree. When the relative Young's modulus is larger than 4, it is an over erosion degree.

Keywords Abrasive suspension jet · Relative Young's modulus · Kerf depth · Surface roughness

1 Introduction

In recent decades, with the development of the industrial processing field and the higher requirement of processing precision in engineering applications, precision processing technology has developed rapidly. Water jet cutting, one of the precision processing technology, is the best fit for cutting various materials [1, 2] such as hard alloy, ceramic, die steel, high silicon cast iron, and other materials with high hardness [3, 4]. Because of its unique processing characteristics, it also has a better performance for cutting viscoelastic materials such as titanium [5, 6], rubber, and others. The earliest application of water jet is rock breaking. With the improvement of the performance and stability of pressure supply equipment and the addition of abrasive particles, water jet is now also used in the processing of high hardness metals and composite materials. Abrasive water jet (AWJ) cutting is one of the fastest developing new cutting technologies in the world. It is a liquid–solid two-phase medium jet mixed with solid particles and high-speed flow of water [7]. With the addition of abrasives, its cutting performance has been greatly improved [8]. In abrasive suspension jet (ASJ), the abrasive and water are mixed in the abrasive tank first and then enter the nozzle. Compared with AWJ, the mixing effect of ASJ is better and the machining accuracy is higher.

For the cutting performance of AWJ and ASJ, scholars at home and abroad have done a lot of research. Srivastava et al. [9] studied metal matrix hard composites on AWJ cutting engineering. The overall material strength was changed by adjusting the proportion of reinforcement B_4C and Al_2O3 (2–4%). The experimental results showed that through the processing of AWJ, the roughness of all samples is 7–9 μm. There are obvious cutting marks and 1.2–1.8-mm pits on the surface, which are caused by the AWJ pulling out the particles of the reinforcing material rather than cutting. Chen et al. [10] studied the cutting characteristics and mechanism of ASJ cutting Q345 through experiment and simulation. The results showed that for the 80-mesh white corundum selected in the experiment, the kerf depth of Q345 is positively correlated with the jet pressure and there is a threshold

✉ Chuwen Guo
cwguo@cumt.edu.cn

[1] School of Low-carbon Energy and Power Engineering, China University of Mining and Technology, Xuzhou 221116, People's Republic of China

[2] Graduate School of Frontier Sciences, University of Tokyo, Chiba, Japan

pressure which is 15–17 MPa. The velocity of abrasive particles is positively correlated with the material failure ability. Adjusting the erosion angle will change the velocity in the vertical and horizontal directions and the kerf depth of Q345 is the largest when the erosion angle is 80°. Yang and Feng [11] designed a five-level orthogonal experiment of four factors (jet pressure, stand-off distance, feed rate, and abrasive flow) on AWJ cutting CFRP. The results showed that the feed rate has the greatest influence on the cutting quality, and the influence degree of other factors from small to large are jet pressure, abrasive flow, and stand-off distance. Bruno Arab et al. [12] studied the cutting of different rocks by AWJ and characterized the cutting seam through SEM and mechanical analysis. The results showed that the failure mechanism of AWJ is different for different rocks, such as quartz sandstone is damaged by the impact of AWJ while marble is damaged by the abrasion of abrasive particles. Krenicky et al. [13] carried out the experiment of AWJ cutting high wear-resistant steel. Through the experimental data, the linear regression equations of jet pressure, feed rate, abrasive flow and surface roughness *Ra* and *Rz* were established. On this basis, the prediction model of kerf angle about *Ra* and *Rz* were studied. Niranjan et al. [14] carried out the orthogonal experiment of AWJ cutting AZ91 magnesium alloy and proposed a method of measuring the kerf depth with a projector. The experimental results showed that the pressure has the greatest influence on the kerf depth. De Abreu et al. [15] explored the influence of jet pressure, stand-off distance, feed rate, and abrasive flow on the depth and width of initial failure zone through the experiment of cutting agate plate with AWJ. The results showed that the stand-off distance has the greatest influence on the experimental indexes. Armağan and Arici [16] carried out the experiment of cutting glass vinyl ester composites by AWJ. The results showed that the stand-off distance has the greatest influence on the upper notch width, and the stand-off distance is also the most significant factor affecting the surface roughness. Kechagias and Petropoulos [17] investigated the influence of sheet thickness, nozzle diameter, standoff distance, and traverse speed during AWJ of transformation-induced plasticity (TRIP) sheet steels on surface quality characteristics. The regression models obtained from the experimental results can well predict the surface roughness and mean kerf. Armağan [18] studied the effects of inter-stack distance, traverse speed, and abrasive mass flow rate on cutting of St37 steel plates in stacked form with AWJ. The experimental results were analyzed by analysis of variance (ANOVA) and showed that the most effective parameters for surface roughness and kerf width in almost all conditions were abrasive mass flow rate and inter-stack distance, respectively. Santhanakumar et al. [19] studied the effect of AWJ parameters like abrasive grain size, abrasive flow rate, nozzle–workpiece standoff, water pressure, and jet traverse rate on the surface roughness and taper angle of cut produced with ceramic tiles. Taguchi's L_{27} orthogonal array was used for conducting the cutting trials, and a combined technique of gray-based response surface methodology (g-RSM) was disclosed for obtaining the optimal level of AWJ parameters.

It can be seen from the researches that the research on the cutting mechanism of AWJ and ASJ is relatively mature and the application scope of AWJ and ASJ has involved various fields. Most scholars optimized the cutting quality by changing the processing parameters (jet pressure, feed rate, stand-off distance, etc.). A small number of scholars have studied the machining characteristics of various materials and the cutting effects of different types of abrasives. However, there is a lack of research on the cutting performance of the relative situation of abrasive physical parameters and material physical parameters. Because the contribution of abrasives to ASJ of cutting materials is more than 90% [20], the cutting performance depends on the result of the physical process of high-frequency collision between abrasives and materials, and the changes in their physical properties will have a great influence on this physical process. Young's modulus reflects the ability of different materials to resist deformation. In the experiment, it is found that the relative ratio of Young's modulus between abrasives and materials seems to show a good law with the cutting performance of ASJ. Kerf depth and surface roughness are two important standards to measure cutting performance. This paper explored the influence of relative Young's modulus on kerf depth and surface roughness of ASJ through the experimental method.

2 Relative Young's modulus

Figure 1 shows the stress–strain curve of the plastic material. When a material is subjected to a normal stress, it will produce deformation. O-A is a linear elastic deformation zone in which the deformation of the material will return to its original state if the normal stress is removed. The ratio of stress to strain at this zone is the Young's modulus of the material. Young's modulus measures the ability of a material to resist deformation. The larger the Young's modulus, the more difficult the material is to deform.

Qiang et al. [20] analyzed the collision process between abrasive particles and metal surfaces in ASJ from the microscopic point of view and established the mathematical model of impact stress and cutting speed of abrasives on the material. As shown in Fig. 2, the collision process between abrasive particles and material surfaces can be simplified as a special case of the physical process of two balls colliding with each other. According to impact mechanics and Hertz theorem, the impact stress

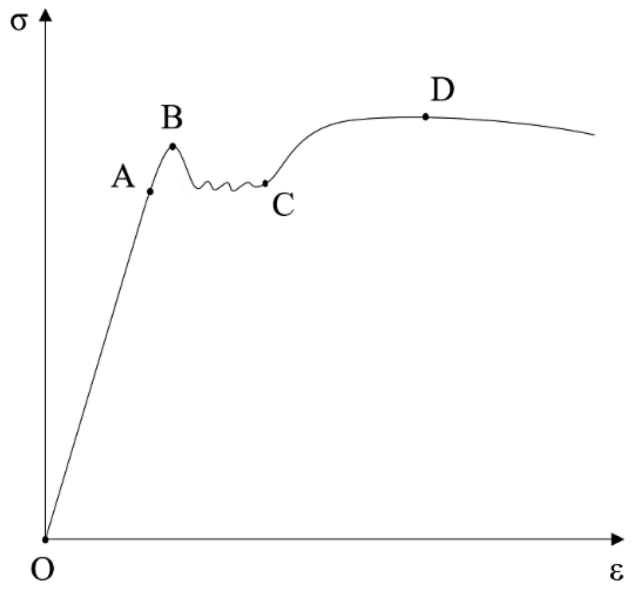

Fig. 1 Stress–strain curve of the plastic material

and the intrusion of the material of this physical process are greatly related to the Young's modulus of the two materials.

For brittle materials (a few cemented carbide, glass, etc.), the larger the hardness and Young's modulus of abrasives, the better the cutting effect will be. This is because the failure of brittle materials is mainly brittle fracture, and according to Hertz theorem, the abrasives with large hardness and Young's modulus have stronger erosion ability and is easier to expand the crack of the materials. For plastic materials (most metals), the larger the hardness and Young's modulus of abrasives, the easier it will intrude, abrade, and remove the materials.

The materials cut by ASJ can be mainly divided into the following types:

1. The material is hard and brittle. The slope of this material in the linear elastic deformation zone (O-A) is large. In other words, its Young's modulus is large. However, this material will directly break after small deformation, and there is no obvious plastic deformation.
2. The material is hard and has high strength. The Young's modulus and breaking strength of this material are relatively large.
3. The material is hard and plastic. This material not only has large Young's modulus and breaking strength but also has large yield stress and fracture elongation. This material is the best material in engineering practice.
4. The material is soft and plastic. The Young's modulus and yield stress of this material are very small, but its fracture elongation is large.

In conclusion, the Young's modulus of abrasive and material will both affect the cutting performance of ASJ. This paper took their relative values as the research object and put forward the concept of relative Young's modulus, which is defined as follows:

$$E_{re} = \frac{E_a}{E_m} \tag{1}$$

where E_a is Young's modulus of abrasive, E_m is Young's modulus of the material.

3 Orthogonal experiment on the influence of relative Young's modulus on ASJ cutting performance

3.1 Design of orthogonal experiment

There are many parameters that affect the cutting performance of ASJ. In order to study the influence of relative

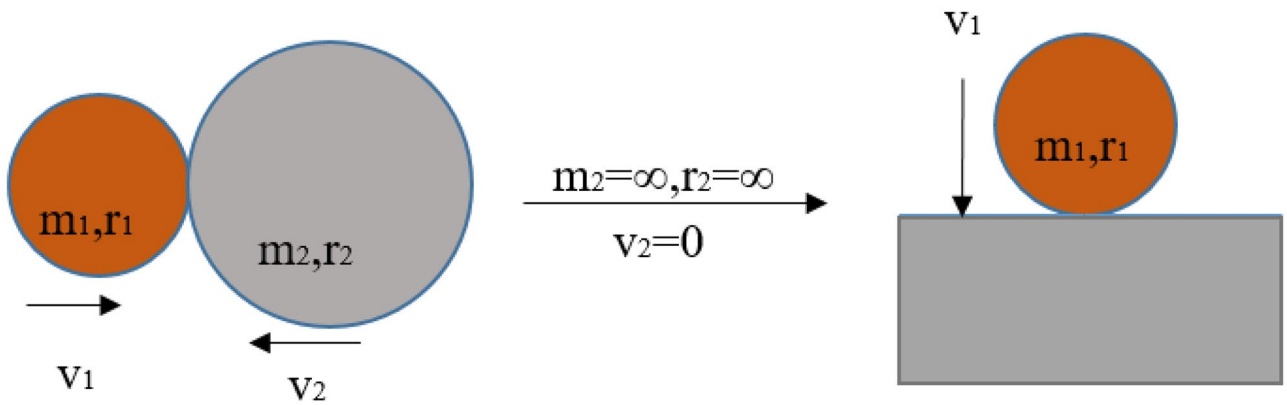

Fig. 2 Simplification of collision physical process [20]

Young's modulus on kerf depth and surface roughness of ASJ. In this experiment, jet pressure and feed rate which also have influence on kerf depth and surface roughness were selected as the comparison. When changing the abrasive, in addition to the Young's modulus, the density and hardness of the abrasive are also changing, and these parameters will interfere with the experimental results. In the orthogonal experiment, different materials will be cut with the same jet parameters while keeping the type of abrasive unchanged.

Garnet was selected as abrasive in this orthogonal experiment. Its composition and physical parameters are shown in Tables 1 and 2. The materials to be cut are 304 stainless steel, TC4 titanium alloy, 7075 aluminum alloy, and AZ31B magnesium alloy. The relative Young's modulus are shown in Table 3. The main experimental equipment includes the Nanjing Dardi water jet cutting platform (Fig. 3) and OLYMPUS super field microscope (Fig. 4). The equipment parameters of the water jet cutting platform are shown in Table 4.

3.2 Orthogonal experimental results and analysis of kerf depth

In this orthogonal experiment, $L_{16}(4^3)$ orthogonal table was used. Combined with equipment conditions and common experimental parameters, the levels of jet pressure, feed rate, and relative Young's modulus in this orthogonal experiment are shown in Table 5. The thickness of the material is 40 mm and the width is 10 mm. In order to avoid the influence of some uncertain factors on the experimental results, each group of experiments was carried out three times, and the experimental results were taken as the average of them.

For the above parameters, L_{16} (4^3) orthogonal table was generated by SPSS software for the experiment.

In this experiment, the kerf depth of the experimental materials could be measured by the measuring tool of the OLYMPUS super field microscope. Table 6 shows the orthogonal experimental data of the kerf depth.

The ANOVA of the experimental results of kerf depth was carried out, as shown in Table 7. The criteria for judging the significance in Table 7 are F(3,6) = 9.78 when $\alpha = 0.01$, F(3,6) = 4.76 when $\alpha = 0.05$, F(3,6) = 3.29 when $\alpha = 0.1$. When the F-value is larger than 9.78, it is considered to be very significant. The main effect plot (MEP) for kerf depth is shown in Fig. 5. The kerf depth is negatively correlated with feed rate and positively correlated with jet pressure and relative Young's modulus. The correlation between kerf depth and relative Young's modulus is better than the other two experimental factors. It can be seen from Table 7 and Fig. 5 that under the conditions of this orthogonal experiment, the relative Young's modulus is more significant on kerf depth than feed rate and jet pressure.

The mathematical model used for kerf depth ANOVA was the linear regression model without interaction products:

$$D_k = -7.83959 - 0.14675R_f + 1.0465P_j + 3.61553E_{re} \pm e \quad (2)$$

where D_k is kerf depth, R_f is feed rate, P_j is jet pressure, E_{re} is relative Young's modulus. D_k's predicted R-sq(pred) is about 97.24% and is close to R-sq(98.54%). The linear regression model can well predict kerf depth under a given independent variable.

When the relative Young's modulus increases, the materials are easier to destroy, the abrasive particles are less likely to disintegrate, and the energy carried by the abrasive particles will be released more thoroughly. In other words, the relative Young's modulus can reflect the "surplus degree" of ASJ cutting. Therefore, the increase of relative Young's modulus will significantly increase the kerf depth.

The function of water jet is to provide velocity for abrasive particles. The larger the jet pressure, the larger the velocity obtained by abrasive particles. According to the momentum theorem, the larger the momentum of a single abrasive particle, the larger the impact energy released when the particle contacts the materials, and the materials are easier to be destroyed and removed. Therefore, when

Table 1 Composition of garnet

Composition	Mass fraction (wt.%)
SiO_2	34–43
FeO	21–36.5
Al_2O_3	18–28
MgO	6–12
Fe_2O_3	6–12
CaO	2–3
MnO	1

Table 2 Physical parameters of garnet

Parameters	Values
Density (kg/m^3)	3800
Mohs hardness (HM)	7.5
Young's modulus (GPa)	248
Poisson's ratio	0.27

Table 3 The relative Young's modulus of materials in orthogonal experiment

Parameters	SS304	TC4	AA7075	MA-AZ31B
Young's modulus (GPa)	194	110	71	48
Relative Young's modulus	1.28	2.25	3.49	5.17

Fig. 3 Nanjing Dardi water jet cutting platform

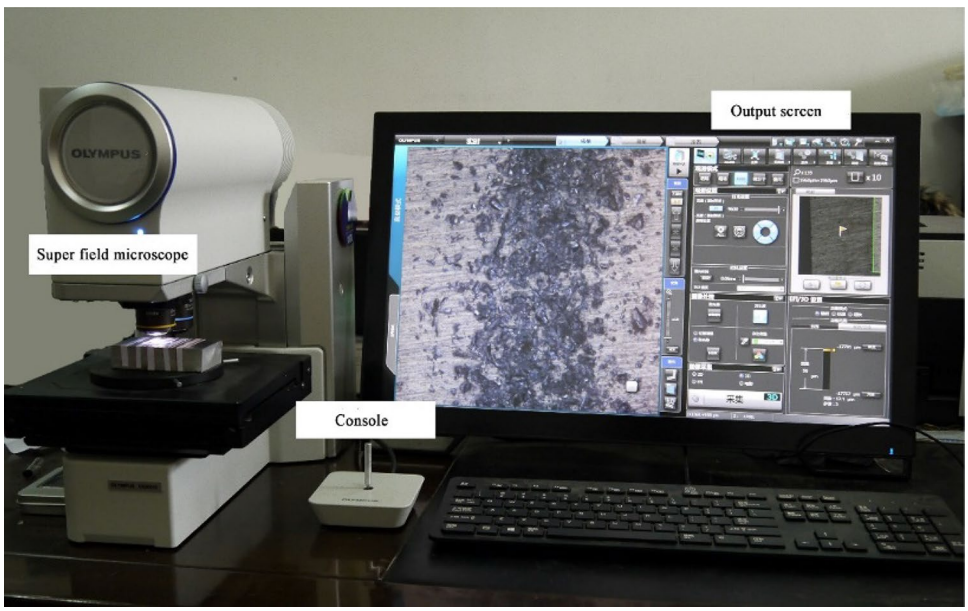

Fig. 4 OLYMPUS super field microscope

Table 4 The equipment parameters of water jet cutting platform (orthogonal experiment)

Parameters	Values
Nozzle length (mm)	79.2
Nozzle outlet diameter (mm)	0.8
Abrasive particle size (mesh)	80
Cutting angle (degree)	0
Stand-off distance (mm)	2

Table 5 Parameter levels of orthogonal experiment (kerf depth)

Parameters	Level 1	Level 2	Level 3	Level 4
Jet pressure (MPa)	12	14	16	18
Feed rate (mm/min)	40	50	60	70
Relative Young's modulus	1.28	2.25	3.49	5.17

Table 6 The orthogonal experimental data of the kerf depth

Serial number	Feed rate levels (mm/min)	Jet pressure levels (MPa)	Levels of relative Young's modulus	Kerf depth (mm)
1	40	12	5.17	17.56
2	40	14	1.28	6.06
3	40	16	3.49	15.54
4	40	18	2.25	13.52
5	50	14	5.17	18.89
6	50	12	1.28	2.97
7	50	18	3.49	15.68
8	50	16	2.25	8.56
9	60	16	5.17	18.48
10	60	18	1.28	6.66
11	60	12	3.49	7.25
12	60	14	2.25	6.04
13	70	18	5.17	20.76
14	70	16	1.28	3.50
15	70	14	3.49	8.17
16	70	12	2.25	3.24

the jet pressure increases, the kerf depth will increase. For ASJ, jet pressure is also the factor restricting its development. Due to the pressure limit of abrasive tank, the maximum pressure that ASJ can reach is about 120 MPa at present, which makes it difficult to realize the cutting of thick and hard materials in some specific environments only by increasing the jet pressure (such as the cutting of tungsten steel wall of nuclear island of nuclear power plant).

Under a given stand-off distance, the diameter of the jet can be regarded as a fixed value. It is advisable to set the diameter of the jet as D. In this experiment, the cutting path is a straight line and then the feed rate can be set as V. It is easy to calculate that the cutting time of ASJ to a certain point on the materials is D/V. When the feed rate becomes smaller, the impact time of the jet and abrasive particles on the same point becomes longer, which means that more abrasive particles impact the same part of the materials, so the kerf depth will become larger. However, if the feed rate is continuously reduced in order to obtain a larger kerf depth, the cutting efficiency will be reduced.

3.3 Orthogonal experimental results and analysis of surface roughness

To ensure that the materials can be cut through by ASJ, the thickness of the material is 20 mm and the width is 10 mm. The parameter levels of orthogonal experiment of surface roughness were determined through pre-experiment, as shown in Table 8.

For the above parameters, L_{16} (4^3) orthogonal table was generated by SPSS software for the experiment. After the experiment, the surface roughness could be measured by the measuring tool of the OLYMPUS super field microscope. The objective lens is 10 × while the eye lens is the system default, and the zoom multiple is 1. In this case, the size of the picture taken by each lens is 1960 μm × 1960 μm and the magnification is 139. The final output picture is composed of

Table 7 ANOVA of kerf depth

Source	DF	Adj SS	Adj MS	*F*-value	*P*-value	%
Feed rate (mm/min)	3	44.433	14.811	0.331	0.803	7.57
Jet pressure (MPa)	3	88.266	29.422	0.716	0.561	15.03
Relative Young's modulus	3	446.024	148.675	13.163	0.000	75.96
Error	6	8.47	0.7062			1.44
Total	15	587.193				100
R-sq						98.54
R-sq(adj)						98.18
R-sq(pred)						97.24

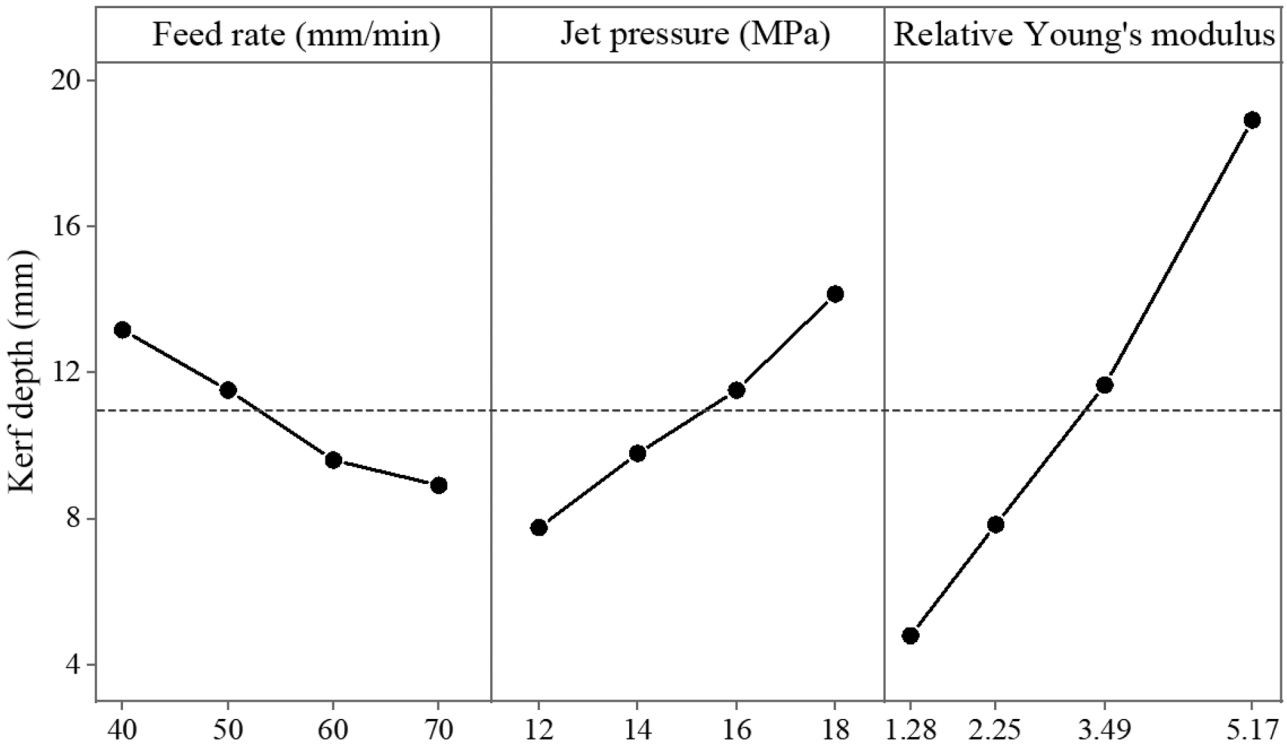

Fig. 5 MEP for kerf depth

several small-size pictures. The sampling method is shown in Fig. 6. Three rectangular areas (front, middle, and rear) were taken for each surface as sample areas, and the size of each sample area is 3 mm × 9 mm. Ten parallel equidistant lines were taken in each sample area as sample lines, and the surface roughness of each sample area was taken by the average of 10 line roughness. The surface roughness of the section was taken as the average of the surface roughness of the three sample areas. The experimental data of surface roughness are shown in Table 9.

The ANOVA of the experimental results of surface roughness was carried out, as shown in Table 10. The criteria for judging the significance in Table 10 are: $F(3,6) = 9.78$ when $\alpha = 0.01$, $F(3,6) = 4.76$ when $\alpha = 0.05$, $F(3,6) = 3.29$ when $\alpha = 0.1$. When the F-value is larger than 4.76 and smaller than 9.78, it is considered to be significant. The MEP for surface roughness is shown in Fig. 7. With the increase of feed rate, jet pressure, and relative Young's modulus, the surface roughness increases as a whole, and they all have a local minimum value in different experimental factors (20 mm/min feed rate, 24 MPa jet pressure, or 2.25 relative Young's modulus). In general, the correlation between surface roughness and relative Young's modulus is the best. It can be seen from Table 10 and Fig. 7 that under the conditions of this orthogonal experiment, the relative Young's modulus is more significant on surface roughness than feed rate and jet pressure.

Table 8 Parameter levels of orthogonal experiment (surface roughness)

Parameters	Level 1	Level 2	Level 3	Level 4
Jet pressure (MPa)	22	24	26	28
Feed rate (mm/min)	15	20	25	30
Relative Young's modulus	1.28	2.25	3.49	5.17

The mathematical model used for surface roughness ANOVA was the linear regression model without interaction products:

$$R_a = 1.42419 + 0.008265R_f + 0.019587P_j + 0.118817E_{re} \pm e \quad (3)$$

R_a's predicted R-sq(pred) is about 47.08% and is far away from R-sq(69.65%). This means that the D_k predictions will be more accurate than the R_a predictions.

With the increase of relative Young's modulus, the surface roughness first decreases and then increases. When the relative Young's modulus is small (at this case, the difference between the Young's modulus of abrasive and material is small), the ability of abrasive particles to remove materials is very poor. This causes the deterioration of the cutting quality of the cutting surface, and there will be more serious trailing in the lower half. Therefore, the surface roughness increases with the relative Young's modulus in this case. When the relative Young's modulus

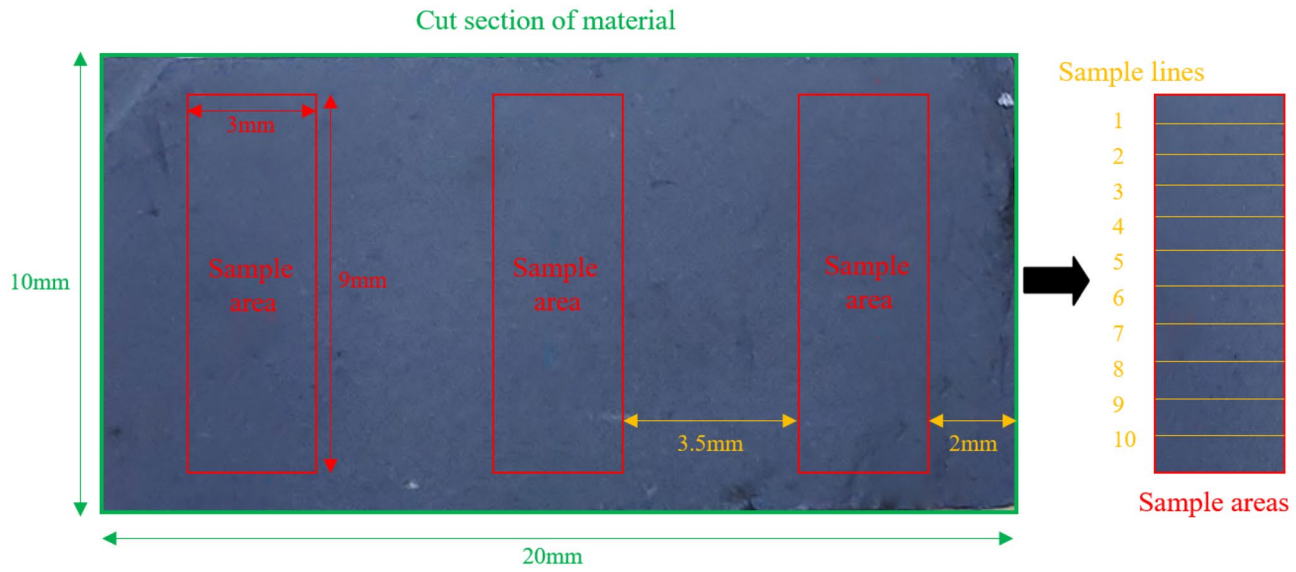

Fig. 6 Sampling method of orthogonal experiment of surface roughness

Table 9 The orthogonal experimental data of surface roughness

Serial number	Feed rate levels (mm/min)	Jet pressure levels (MPa)	Levels of relative Young's modulus	Surface roughness (μm)
1	15	22	1.28	2.256
2	15	24	2.25	2.226
3	15	26	3.49	2.612
4	15	28	5.17	2.742
5	20	24	1.28	2.047
6	20	22	2.25	2.171
7	20	28	3.49	2.466
8	20	26	5.17	2.803
9	25	26	1.28	2.396
10	25	28	2.25	2.157
11	25	22	3.49	2.562
12	25	24	5.17	2.663
13	30	28	1.28	2.507
14	30	26	2.25	2.562
15	30	24	3.49	2.572
16	30	22	5.17	2.649

Table 10 ANOVA of surface roughness

Source	DF	Adj SS	Adj MS	*F*-value	*P*-value	%
Feed rate (mm/min)	3	0.083	0.028	0.475	0.706	8.7
Jet pressure (MPa)	3	0.109	0.036	0.650	0.598	11.43
Relative Young's modulus	3	0.525	0.175	8.247	0.003	55.06
Error	6	0.2365	0.0197			24.8
Total	15	0.9535				100
R-sq						69.65
R-sq(adj)						62.06
R-sq(pred)						47.08

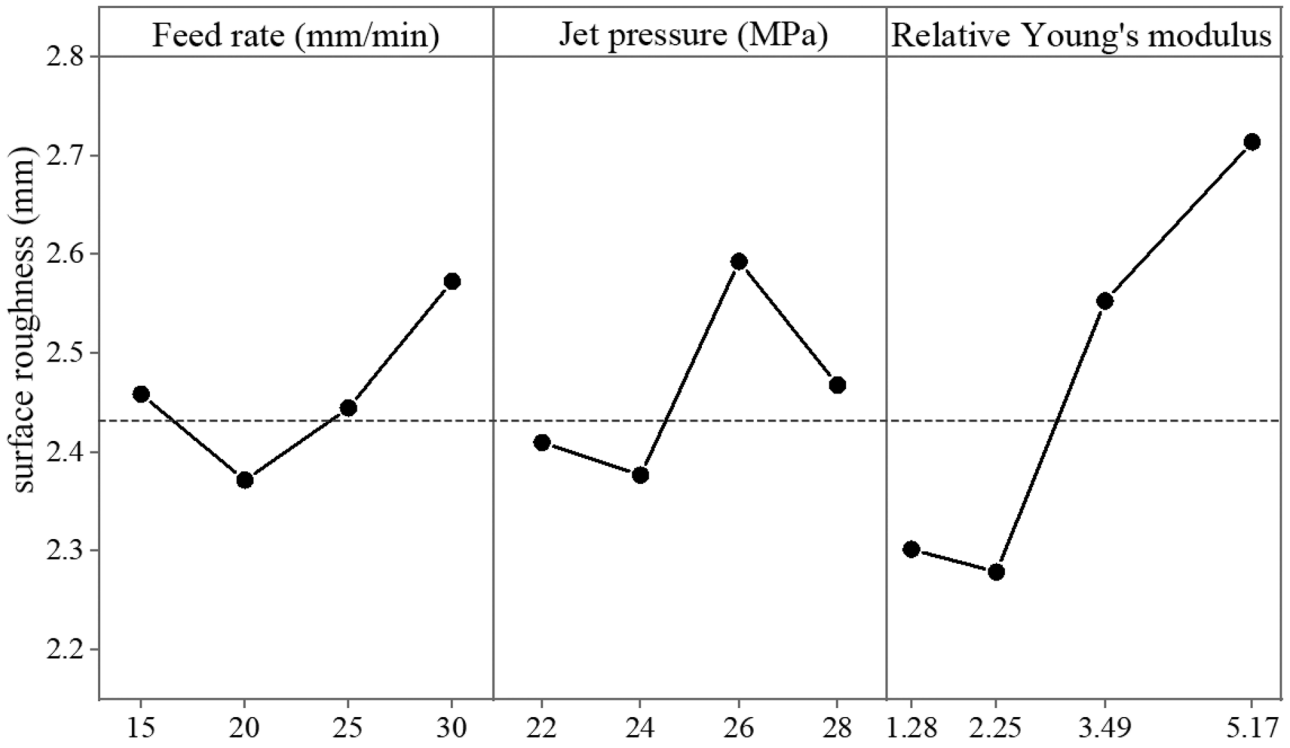

Fig. 7 MEP for surface roughness

reaches a certain critical value, the surface roughness decreases with its increase. The reason is that in this case, the "surplus degree" of abrasive particles to remove materials has been very large. If the relative Young's modulus continues to increase, abrasive particles will be easier to leave deep and long scratches on the cutting surface, resulting in poor cutting quality.

With the increase in feed rate, the surface roughness first decreases and then increases. This is because when the feed rate becomes smaller, the abrasive particles impact the same position for a longer time, and the subsequent abrasive particles can polish the cutting surface, which makes cutting quality better. However, when the feed rate decreases to a certain critical value, continuing to reduce the feed rate will deteriorate the cutting quality. Excessive repeated impact at the same position will produce deep scratches and increase the surface roughness.

The influence of jet pressure on surface roughness is similar to that of feed rate, and the best surface roughness appears at a certain value. When the jet pressure is too small, the impact capacity of abrasive particles is insufficient, which will cause more serious tailing and larger surface roughness. When the jet pressure is too large, the material surface will be impacted excessively, resulting in large surface roughness.

4 Single factor experiment on the influence of relative Young's modulus on ASJ cutting performance

4.1 Design of single factor experiment

The results of orthogonal experiments showed that the relative Young's modulus can significantly affect the kerf depth and surface roughness of ASJ. On this basis, this paper quantitatively studied the changes in kerf depth and surface roughness with relative Young's modulus by a single factor experiment. In the orthogonal experiment, in order to reduce the influence of the change of other physical parameters of the abrasive on the significance, only garnet was used as the abrasive. In order to ensure the objectivity of the experimental results, garnet, white corundum, and silicon carbide were used in the single factor experiment. At the same time, the range of processed materials was expanded. Copper alloy, glass, and tungsten steel with larger Young's modulus and brittleness were added.

White corundum is one of the corundum abrasives with high purity. High purity aluminum oxide powder (the content of Al_2O_3 is generally more than 98%) turns into

Table 11 Composition of white corundum

Composition	Mass fraction (wt.%)
Al_2O_3	> 99.6
Na_2O	< 0.4

Table 12 Physical parameters of white corundum

Parameters	Values
Density (kg/m^3)	3950
Mohs hardness (HM)	9
Young's modulus (GPa)	350

Table 13 Composition of silicon carbide

Composition	Mass fraction (wt.%)
SiC	> 98.5
C (Free state)	< 0.2
Fe_2O_3	< 0.6

Table 14 Physical parameters of silicon carbide

Parameters	Values
Density (kg/m^3)	3200
Mohs hardness (HM)	9.5–9.8
Young's modulus (GPa)	450
Poisson's ratio	0.31

a molten state after high temperature, and it cools and crystallizes to form white corundum. Alumina powder is made of bauxite through a series of refining and processing. In the process of preparing alumina powder, a certain amount of impurity Na_2O will be produced. This material will evaporate under high temperatures and produce pores in white corundum crystal. These pores cause white corundum to be hard and brittle. Composition and physical parameters of white corundum are shown in Tables 11 and 12.

The main raw material of silicon carbide is quartz sand. Other materials include oil, coke, and sawdust. They are smelted together in a resistance furnace with a high temperature of thousands of degrees. Composition and physical parameters of silicon carbide are shown in Tables 13 and 14.

The particle size of the abrasive particles set in the experiment is 80 mesh. In order to ensure that the particle sizes of the three abrasives are basically the same, large particles and impurities in the original abrasives were filtered out to avoid blocking the nozzle. In this experiment, 70-mesh and 80-mesh sieves were selected to filter the original 80-mesh abrasives. The filtered abrasive particles were used as standard size abrasives in this experiment.

Materials of single factor experiment include stainless steel (304), titanium alloy (TC4), aluminum alloy (7075), magnesium alloy (AZ31B), tungsten steel (YG20 and YG8), brass (H62), and glass. Their relative Young's modulus are shown in Table. 15. The equipment parameters of water jet cutting platform are shown in Table. 16.

4.2 Single factor experimental results and analysis of kerf depth

In this experiment, the thickness of the material is 40 mm and the width is 10 mm. In order to avoid the influence of some uncertain factors on the experimental results, each group of experiments was carried out three times, and the experimental results were taken as the average of them.

Figure 8 shows the change law of ASJ kerf depth with relative Young's modulus. It can be seen from Fig. 8 that the kerf depth of materials is positively correlated with relative Young's modulus, and the correlation is good.

According to the trend of the curve, it can be calculated that generally under the same relative Young's modulus, the kerf depth white corundum > garnet > silicon carbide. The values of white corundum are 15–42% larger than that of garnet and 20–100% larger than that of silicon carbide. The reason is that the density of white corundum is the largest. Under the same other conditions, it obtains the largest kinetic energy and has the greatest impact on the materials. Therefore, most materials can be removed at the same time and the kerf depth is the largest. The density of silicon carbide is the smallest, so the kerf depth is also the smallest. However, this law is different when the

Table 15 The relative Young's modulus of materials in single factor experiment

Relative Young's modulus	Yg8	Yg20	SS304	TC4	H62	AA7075	Glass	AZ31B
Young's modulus of material	510	390	194	110	102	71	55	48
Garnet	0.49	0.64	1.28	2.25	2.43	3.49	4.51	5.17
White corundum	0.69	0.90	1.80	3.18	3.43	4.93	6.36	7.29
Silicon carbide	0.88	1.15	2.32	4.09	4.41	6.34	8.18	9.38

Table 16 The equipment parameters of water jet cutting platform (single factor experiment)

Parameters	Values
Nozzle length (mm)	79.2
Nozzle outlet diameter (mm)	0.8
Abrasive particle size (mesh)	80
Abrasive types	Garnet, white corundum, silicon carbide
Cutting angle (degree)	0
Feed rate for experiment of kerf depth (mm/min)	60
Feed rate for experiment of surface roughness (mm/min)	20
Jet pressure for experiment of kerf depth (MPa)	15
Jet pressure for experiment of surface roughness (MPa)	28
Stand-off distance (mm)	2

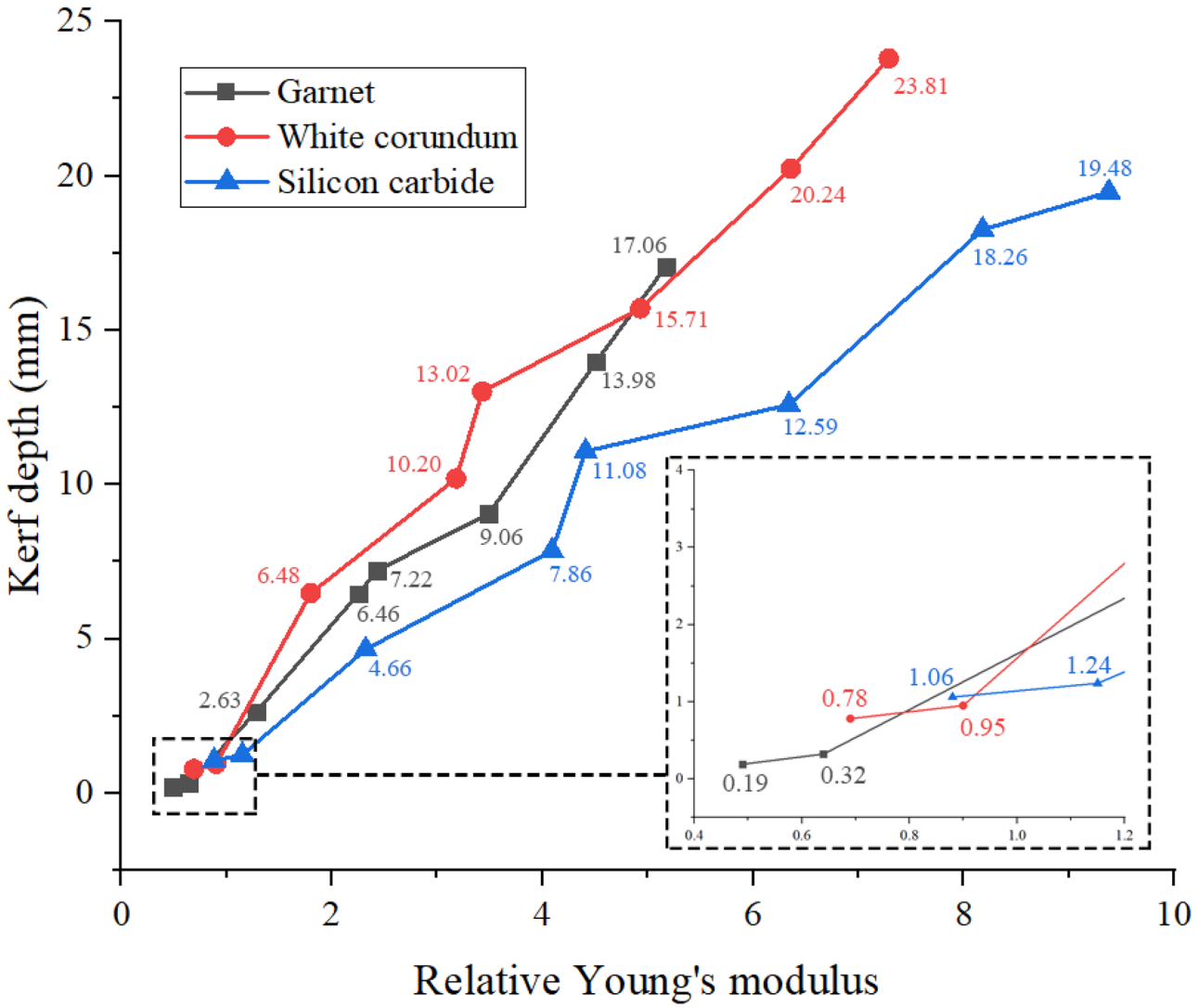

Fig. 8 The change law of ASJ kerf depth with relative Young's modulus

materials are tungsten steel Yg8 and Yg20. For Yg8 and Yg20, silicon carbide can cause more kerf depth than white corundum and garnet. The values of silicon carbide are 30–36% larger than that of white corundum and 288–458% larger than that of garnet. It is worth noting that the relative Young's modulus of white corundum and garnet to tungsten steel is smaller than 1. Because the Young's modulus of silicon carbide is larger than that of white corundum and garnet, the relative Young's modulus of silicon carbide to tungsten steel is close to 1 or even larger than 1. The relative Young's modulus can reflect the "surplus degree" of ASJ cutting. When the relative Young's modulus is larger than 1, the abrasives are always surplus for cutting materials. In this case, the influence of density on kerf depth is more than that of relative Young's modulus. When the relative Young's modulus is smaller than 1, the abrasives are not surplus for cutting materials. The abrasive particles will become easier to break, and the materials will be more difficult to remove. In this case, the relative Young's modulus has a greater influence on the kerf depth than density.

4.3 Single factor experimental results and analysis of surface roughness

In this experiment, the thickness of the material is 10 mm and the width is 20 mm. The surface roughness *Ra* was used as the standard to measure the cutting quality. *Ra* refers to the mean arithmetic deviation of contour. Within the range of evaluation length *L*, the mean arithmetic of the absolute value of deviation *Z* from each point on the contour line to the baseline is equal to *Ra*. The definition method of *Ra* is shown in Fig. 9, and the calculation formula can be given by:

$$\begin{aligned} Ra &= \frac{1}{L}\int_0^L |z-m|dx \\ m &= \int_0^L zdx \end{aligned} \tag{4}$$

The sampling method used in the single factor experiment is similar to that used in the orthogonal experiment, as shown in Fig. 10. Take the sampling area 1–3 mm away from the upper edge of the cutting as the upper roughness, and take the sampling area 7–9 mm away from the upper edge of the cutting as the lower roughness. The surface roughness was measured with a linear roughness measuring tool of the super field microscope. In each sampling area, take 5 parallel straight lines as sample lines to measure the line roughness, and use the average line roughness of these 5 lines as the surface roughness of the sampling area.

Figure 11 shows the change of surface roughness with relative Young's modulus (garnet). Under the parameters of this experiment, the two tungsten steels were not cut through by garnet, so there is no data on the surface roughness of the two tungsten steels. As can be seen from Fig. 11, the upper and lower surface roughness of the material first decreases and then increases with the increase of the relative Young's modulus. The change trend of the surface roughness turns when the relative Young's modulus is 2.25. When the relative Young's modulus is very small, the lower roughness will be very large (20.05% larger than the upper roughness). When the relative Young's modulus is larger than or equal to 2.25, the lower roughness is 3.53% larger than the upper roughness on average.

Figure 12 shows the change law of surface roughness with relative Young's modulus (white corundum). For white corundum, tungsten steel Yg20 was cut through under the experimental parameters while tungsten steel Yg8 was not completely cut through, so there is no data on the surface roughness of Yg8. It can be seen from Fig. 12 that the law of white corundum is similar to that of garnet. With the increase of relative Young's modulus, the upper and lower surface roughness of the material first decreases and then increases. The change trend of surface roughness turns when the relative Young's modulus is 1.8, and the rising rate after turning is

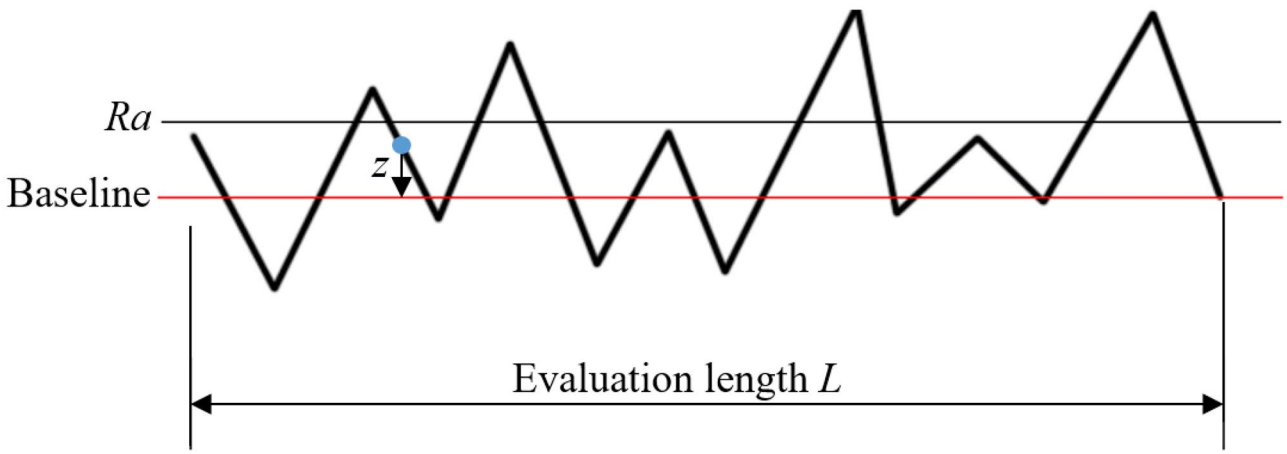

Fig. 9 The definition method of *Ra*

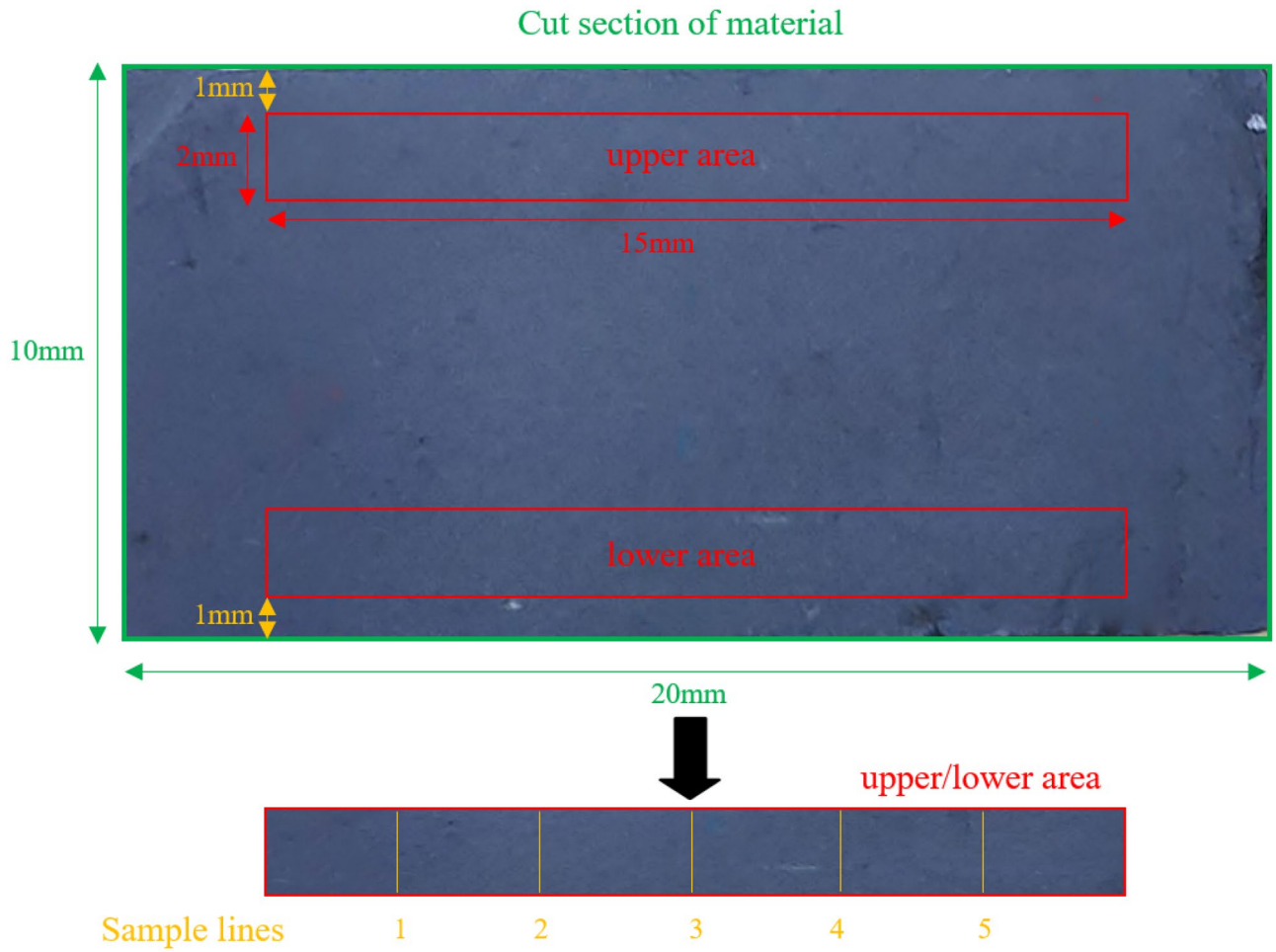

Fig. 10 Sampling method of single factor experiment of surface roughness

larger than that of garnet. When the relative Young's modulus is very small, the lower roughness will be very large (104.19% larger than the upper roughness). When the relative Young's modulus is larger than or equal to 1.8, the lower roughness is 5.05% larger than the upper roughness on average.

Figure 13 shows the change law of surface roughness with relative Young's modulus (silicon carbide). For silicon carbide, tungsten steel Yg8 is not completely cut through under the parameters of this experiment, so there is no data on the surface roughness of Yg8. It can be seen from Fig. 13 that the law of silicon carbide is also conforms to the trend of the other two abrasives. The change trend of surface roughness turns when the relative Young's modulus is 2.32, and the rising rate after turning is smaller than that of white corundum and larger than that of garnet. When the relative Young's modulus is very small, the lower roughness will be very large (113.80% larger than the upper roughness). When the relative Young's modulus is larger than or equal to 2.32, the lower roughness is 13.26% larger than the upper roughness on average.

Taking the average value of upper roughness and lower roughness as the average surface roughness, Fig. 14 shows the change law of average surface roughness and relative Young's modulus of three different abrasives. As can be seen from Fig. 14, when the relative Young's modulus is smaller than 1.5, the average surface roughness will increase significantly, and the values of garnet are much smaller than that of white corundum and silicon carbide. When the relative Young's modulus is between 1.5 and 4, the average surface roughness of the three abrasives is all very small, and the surface quality of the materials is the best. When the relative Young's modulus is larger than 4, the average surface roughness increases, and the increase rate of white corundum is faster than that of garnet and silicon carbide.

The relative Young's modulus can reflect the "surplus degree" of ASJ cutting. If the relative Young's modulus is too small, the abrasive particles do not have enough energy to polish the cutting surface after removing the materials. If the relative Young's modulus is too large, the surplus

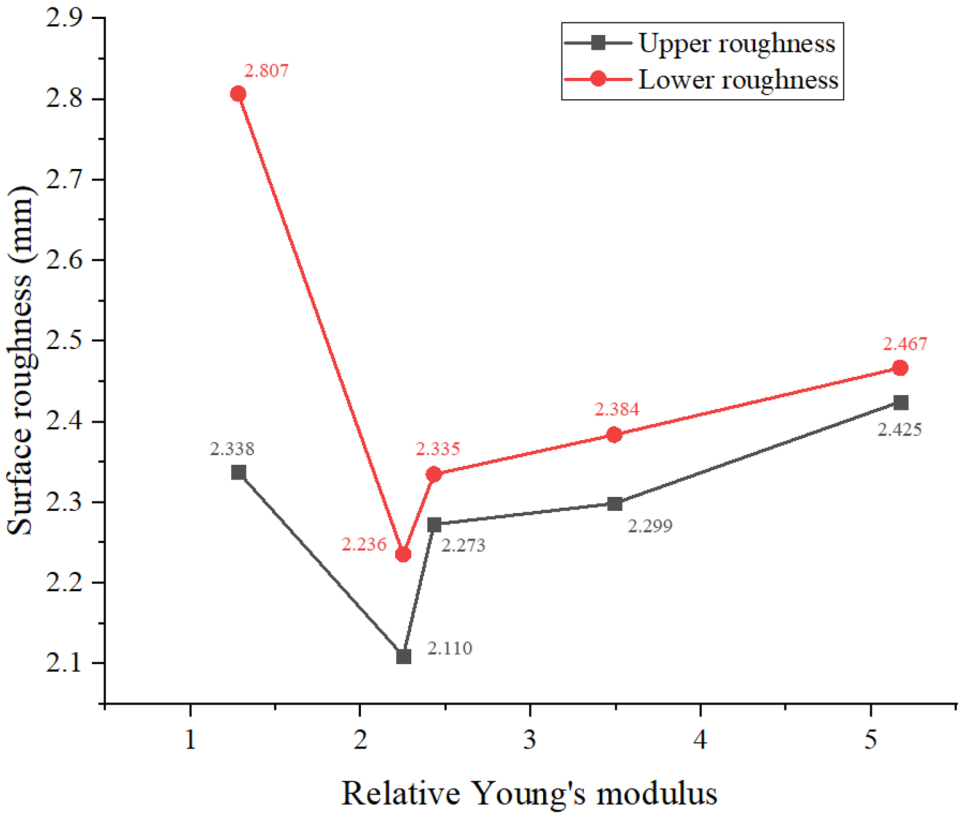

Fig. 11 The change of surface roughness with relative Young's modulus (garnet)

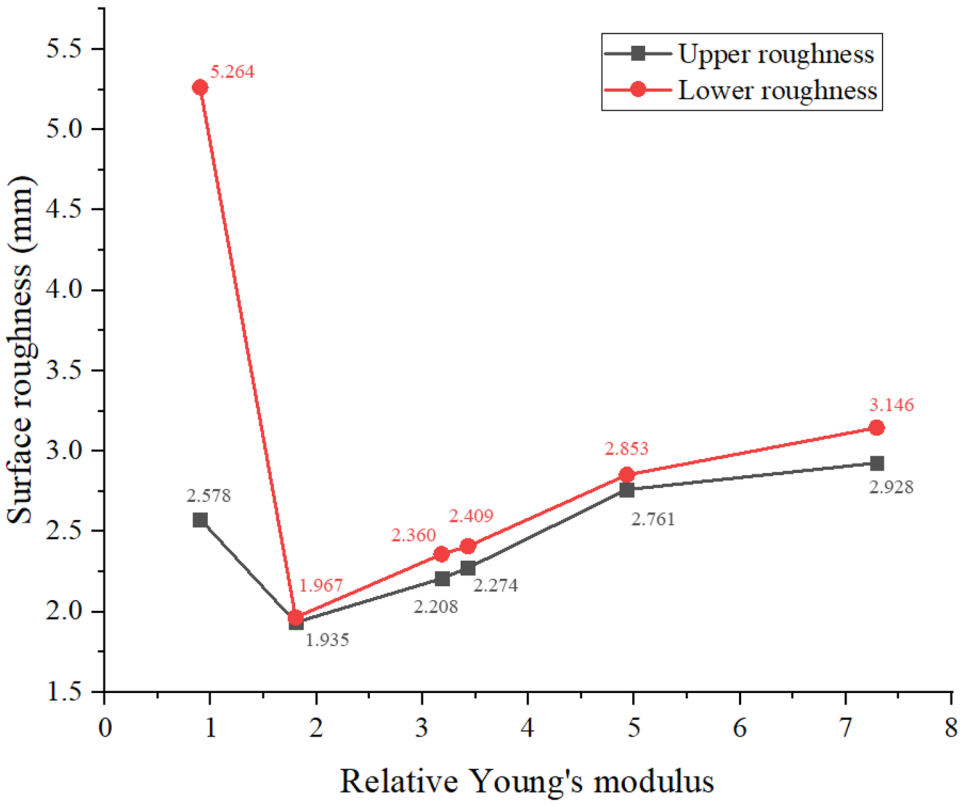

Fig. 12 The change law of surface roughness with relative Young's modulus (white corundum)

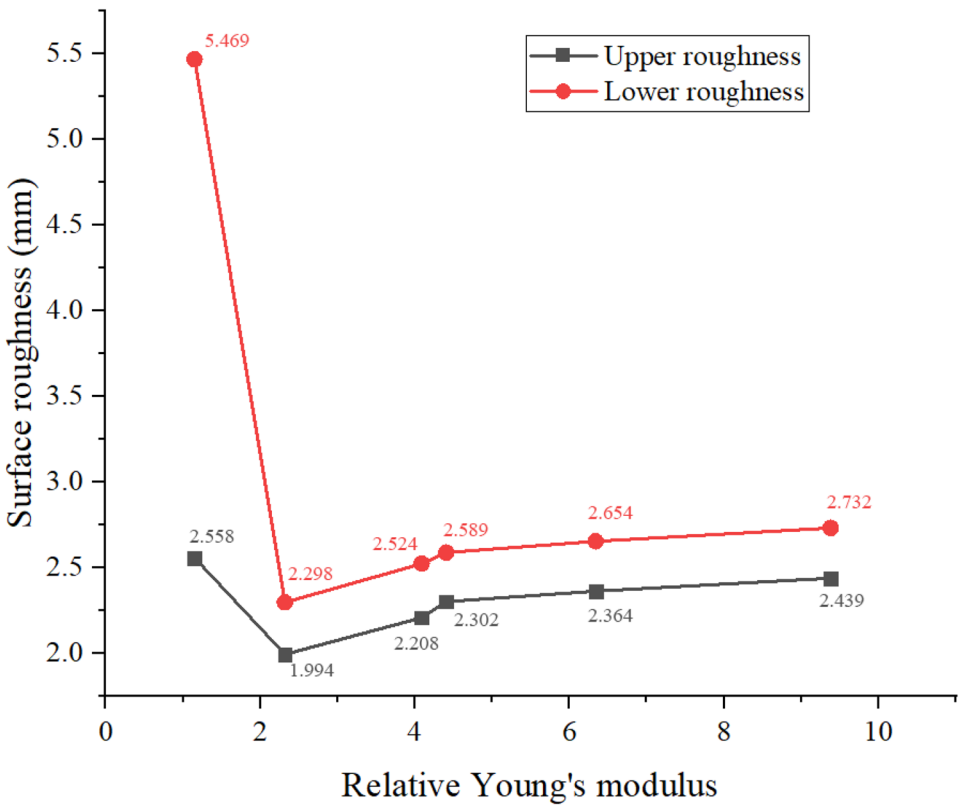

Fig. 13 The change law of surface roughness with relative Young's modulus (silicon carbide)

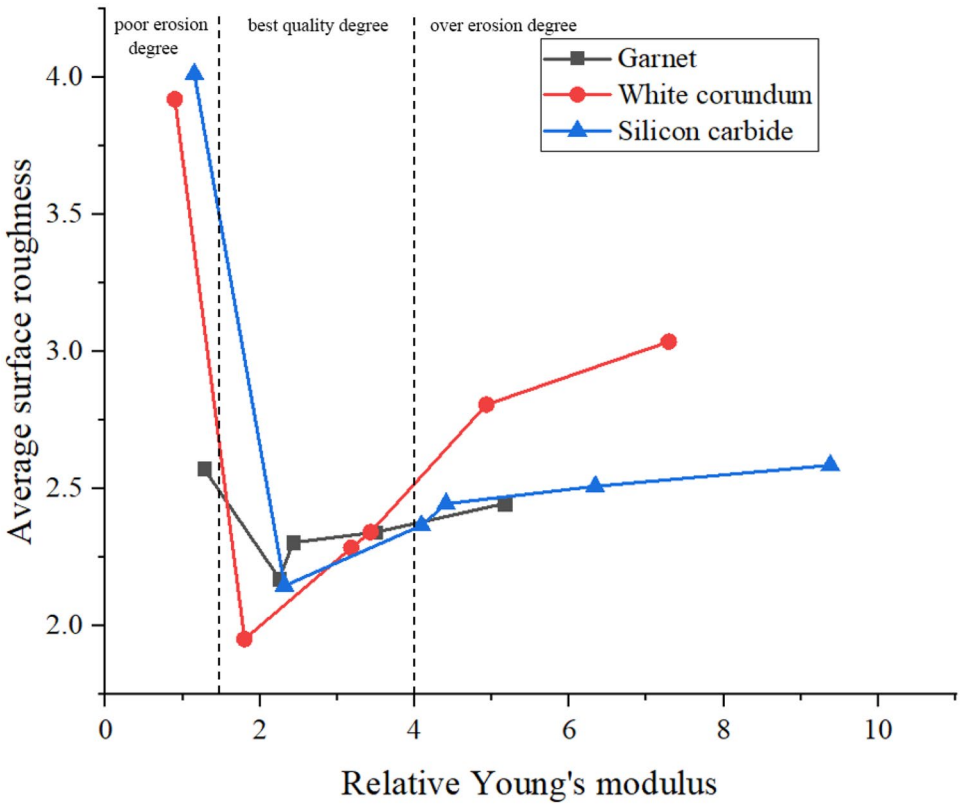

Fig. 14 The change law of average surface roughness and relative Young's modulus of three different abrasives

energy of the abrasive particles after polishing the cutting surface will cause new scratches. Both cases will lead to an increase in surface roughness. According to the experimental results, the cutting quality is divided into three degrees. When the relative Young's modulus is smaller than 1.5, it is a poor erosion degree. When the relative Young's modulus is between 1.5 and 4, it is the best quality degree. When the relative Young's modulus is larger than 4, it is an over erosion degree.

5 Conclusion

Through the research, the following conclusions are drawn:

1. The relative Young's modulus can reflect the "surplus degree" of ASJ cutting. In the parameter range of orthogonal experiment (jet pressure 12–17 MPa for kerf depth and 22-28 MPa for surface roughness, feed rate 40–70 mm/min for kerf depth, and 15–30 mm/min for surface roughness), the influence of relative Young's modulus on cutting performance is more significant than jet pressure and feed rate.
2. When the relative Young's modulus is larger than 1, the influence of abrasive density on kerf depth is greater than that of relative Young's modulus. Therefore, the white corundum with the highest density has more advantages than garnet and silicon carbide in cutting conventional metals and glasses. Kerf depth of white corundum is 15–42% larger than that of garnet and 20–100% larger than that of silicon carbide. When the relative Young's modulus is smaller than 1, the relative Young's modulus has a greater influence on the kerf depth than abrasive density. Therefore, the kerf depth of silicon carbide with the largest Young's modulus is much larger than that of garnet and white corundum in cutting metals with large Young's modulus (Yg8 and Yg20). Kerf depth of silicon carbide is 30–36% larger than that of white corundum and 288–458% larger than that of garnet.
3. The upper and lower surface roughness of the material first decreases and then increases with the increase of the relative Young's modulus. For the same abrasive, the lower roughness is always larger than the upper roughness. When the relative Young's modulus is very small, the lower roughness will be very large (20.05–113.80% larger than the upper roughness at different abrasives). Garnet has the smallest surface roughness when the relative Young's modulus is small, and the surface roughness of white corundum increases rapidly when the relative Young's modulus is large.
4. The three abrasives have their own advantages and disadvantages in different aspects. The choice of abrasives for ASJ cutting different materials can be determined according to the relative Young's modulus. When the relative Young's modulus is smaller than 1, in order to improve the cutting efficiency, the abrasive with larger Young's modulus (silicon carbide) should be selected. When the relative Young's modulus is between 1 and 1.5, smaller surface roughness can be obtained by cutting with garnet as abrasive. When the relative Young's modulus is between 1.5 and 4, using white corundum as abrasive for cutting can obtain the maximum kerf depth without large surface roughness.

Author contribution Chiheng Qiang conceived of the study, designed the study, and wrote the manuscript. All authors were involved in collecting and analyzing the data, also revisions.

Funding This study was funded by the National Natural Science Foundation of China (Grant No: 52104150), the Natural Science Foundation of Jiangsu Province (Grant No: BK20200657) and Hebei Natural Science Foundation Ecological Wisdom Mine Joint Fund Project (Grant No: E2020402075).

Data availability The data sets supporting the results of this article are included within the article and its additional files.

Declarations

Ethics approval Not applicable.

Consent to participate Not applicable.

Consent for publication All authors agree to transfer copyright of this article to the Publisher.

Competing interests The authors declare no competing interests.

References

1. Hashish M (1991) Characteristics of surface machined with abrasive water jet. J Eng Mater Technol ASME 113:354–362
2. Hashish M (1988) Visualization of surfaces machined with abrasive water jet cutting process. Exp Mech 28:159–168
3. Yang Z, Chen SM, Zhang YJ, Li M (2009) Development and application of high pressure water jet technology. Mech Manag Dev 24:87–90 (in Chinese with English abstract)
4. Feng YX (2007) Abrasive water jet milling ceramic materials processing technology research. Dissertation, Shandong Univ (in Chinese with English abstract)
5. Wang YW (2013) Abrasive water jet cutting titanium alloy experimental study. Dissertation, Xihua Univ (in Chinese with English abstract)
6. Rongrun R (2002) Current status and development trend of water jet processing technology. Aviat Precis Manuf Technol 38:12–14
7. Momber AW, Kovacevic R (1998) Principles of abrasive water jet machining. Springer, London. https://doi.org/10.1007/978-1-4471-1572-4
8. Wang FC, Zhou DP, Xu QW, Qiang CH, Guo CW (2018) Mathematical model of rock stress under abrasive slurry jet impact based on contact mechanics. Int J Rock Mech Min 107:1–8

9. Srivastav AK, Dwivedi SP, Maurya NK, Sahu R (2020) Surface roughness report and 3D surface analysis of hybrid metal matrix composites (MMC) during abrasive water jet (AWJ) cutting. Rev Compos Mater Av 30(3–4)
10. Chen X, Guan J, Deng S, Qiang L, Ming C (2018) Features and mechanism of abrasive water jet cutting of Q345 steel. Heat Technol 36(1):81–87
11. Yang G, Feng B (2020) Orthogonal experiment on the surface quality of carbon Fiber reinforced plastic cut by abrasive water jet. Rev Compos Mater Av 30(2):69–76
12. Bruno Arab P, Barreto Celestino T (2020) A microscopic study on kerfs in rocks subjected to abrasive waterjet cutting. Wear 448–449:203–210
13. Krenicky T, Servatka M, Gaspar S, Mascenik J (2020) Abrasive water jet cutting of hardox steels-quality investigation. Processes 8(12):1652. https://doi.org/10.3390/pr8121652
14. Niranjan CA, Srinivas S, Ramachandra M (2018) An experimental study on depth of cut of AZ91 magnesium alloy in abrasive water jet cutting. Mater Today: Proc 5(1):2884–2890
15. De Abreu E, Lima Ipar CE, Neis PD, Ferreira NF, Lasch G, Zibetti TF (2020) Analysis of the initial damage region in agate plates cut by abrasive waterjet (AWJ) process. Int J Adv Manuf Technol 109(9–12):2629–2638
16. Armağan M, Arici AA (2017) Cutting performance of glass-vinyl ester composite by abrasive water jet. Mater Manuf Processes 32(15):1715–1722
17. Kechagias J, Petropoulos G (2012) Application of Taguchi design for quality characterization of abrasive water jet machining of TRIP sheet steels. Int J Adv Manuf Technol 62(5–8):635–643
18. Armağan M (2021) Cutting of St37 steel plates in stacked form with abrasive water jet. Mater Manuf Process 36(11):1305–1313
19. Santhanakumar M, Adalarasan R, Rajmohan M (2015) Experimental modelling and analysis in abrasive waterjet cutting of ceramic tiles using grey-based response surface methodology. Arab J Sci Eng 40(11):3299–3311
20. Qiang CH, Wang FC, Guo CW (2019) Study on impact stress of abrasive slurry jet in cutting stainless steel. Int J Adv Manuf Technol 100(1–4):297–309